Egyptian Geophysical Society
EGS Journal, Vol. 9, No. 1, 127-133 (2011)

APPLICATION OF AUTOMATIC EXTRACTION OF LINEAMENT FEATURES FROM GEOPHYSICAL DATA IN SELECTED AREA

A.A. Khamies, A.I. Kamel and R.M. Mohamed
Nuclear Material Authority, P.O. Box 530, Maadi, Cairo, Egypt.

تطبيق طريقة الاستخراج التلقائى للملامح الخطية من البيانات الجيوفيزيقية على منطقة مختارة

الخلاصة: يقدم العمل الحالى عدة طرق رياضية لاستنتاج الملامح الخطية مباشرة من البيانات الجيوفيزيقية وتطبيقها على منطقة مختارة. لقد تم تصميم ثلاثة طرق تنفذ متتالية لتحقيق هذا الغرض حيث تعطى الأولى التفاضل الثانى لبيانات الجهد مما يظهر الملامح الخطية ثم تعين الثانية احداثيات (نقطتى البداية و النهاية) و طولها. أخيرا يتم ترتيب و جدولة و رسم الشكل الوردى لهذه الملامح الخطية وفق عددها أو أطوالها أو نسبها. تم اختبار مدى صلاحية الطريقة المقترحة باستخدام بيانات تخليقية وحقلية حيث طبقت على بيانات الجاذبية لمنطقة الواحات الخارجة وتبين من وجود مجموعات من الصدوع تأخذ الاتجاه (شمال شرق الى شرق الشمال الشرقى وغرب الجنوبى الشرقي) تتحكم فى الإطار التركيبى .

ABSTRACT: *The present work provides an application of new algorithms to estimate lineaments directly from geophysical data in selected area.. Three algorithms were designed and used to accomplish these goals where gradient filters (derivative) were used first to emphasize the long linear features of potential data.*
The second algorithm was used to define the lineament coordinates (start and end points), and the last one was applied to count and tabulate the extracted lineaments and finally represent it either in frequency and/or number. The proposed method is tested using theoretical and field examples. EL-Kharga area was utilized to test the validity of this technique. The most interesting phenomenon is the occurrence of two fault systems running generally in NE-SW to ENE-WSW and ESE-WNW to E-W that affect the studied area.

INTRODUCTION

Lineaments are naturally occurring alignments of soil, topography, stream channels, vegetation, or a combination of these features that are visible on remotely sensed imagery and aerial photographs. Many lineaments are believed to be directly related to tectonic activity or tectonic features (Rowan and Lathran, 1980). Linear anomalies are critical in the interpretation of gravity and magnetic data (Zhang et. al., 2006). The interpretation of lineaments is subjective and considerable experience is required to see week lineament and to determine their length adequately. It depends on the aeromagnetic map quality, contour interval, and interpreter's judgment.

Several persons should co-operate in the interpretation to obtain the best possible result (Khamies et. al., 2001). In this study the long linear features of potential data were identified by using proper type of derivative filters. Second vertical or directional derivative filter were applied on the potential field data to delineate the lineaments. Lineaments lengths were identified and their orientations were compared to known subsurface geologic structural features in the area. The final product is creating a rose diagram from azimuth bearing or line endpoints data.

LINEAMENT IDENTIFICATION

(FILTER DESIGN)

The second horizontal gradient techniques is a tool to process and interpret field data from magnetic and gravity surveys. Early papers, such as Evjen (1936) and Heiland (1943), emphasize the role of gravity gradients in structural interpretation of gravity data. Several authors were devoted exclusively to the theory, measurement, and applications of gravity gradients; i.e., Mueller (1960), Trommer (1964), Beyer (1971), and Butler (1983). Numerous publications describe procedures for calculating gravity gradients and higher-order derivatives from measured gravity data using various "center point and ring" numerical filtering methods (e.g., Agarwal and Lal, 1972a,b; Baranov, 1975). Recent papers, such as Nabighian (1984), Moon et al. (1988), Pederson (1989), and Khamies (2004) emphasize the usefulness of spatial gradients for potential field analysis in general. Many authors have explored the use of gravity gradients for detailed 2-D structural interpretation of the truncated plate model; for example, Hammer and Anzoleaga (1975), Green (1976), Stanley and Green (1976), Stanley (1977), and Klingele et al. (1991). Other authors, such as Fajklewicz (1976) and Butler (1984b), have used the delectability and resolution advantages of gravity gradients for detection and mapping of shallow geologic and cultural features.

Suppose that, we have 5 data points and wish to fit the observed data, in some sense, by the following second order polynomial

$$F = a_0 + a_1 x + a_2 x^2 \qquad (1)$$

Where a_0 , a_1 and a_2 are the coefficients to be determined.

Consider that, we have a set of five equal data points as shown in Fig.(l). If we fit this data by a plane surface polynomial in least-squares sense (eq. l) then, the first and second derivative values of potential field in x direction can be represented by the equations (2) and (3) respectively.

$$F_x = a_1 + 2a_2 x \quad (2)$$

$$F_{xx} = 2a_2 x \quad (3)$$

Where a_2 is the coefficient of the second horizontal derivative in X direction.

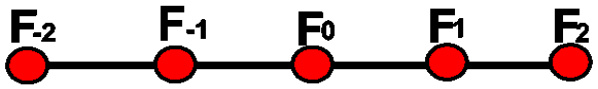

Fig. (1): Five equally spaced data point's filters.

The computations for the above procedure can be relatively easy, if the potential field data function $F(x_i)$ for each value of x and the x's are equally spaced (along profile) and arranged symmetrically around the calculation point i.e. x_i = -2, -1, 0, 1, 2 such that $\sum x_i = 0$. The variables of the equation (1) are the coefficient a_0 , a_1 and a_2 of the plane. To find a minimum, we naturally differentiate F with respect to a_0 , a_1 and a_2 and then set the resulting expressions equal to zero. This process (normalization) gives the following equations (4), (5) & (6) respectively.

$$a_0 n + a_1 \sum x + a_2 \sum x^2 = \sum F \quad (4)$$

$$a_0 \sum x + a_1 \sum x^2 + a_2 \sum x^3 = \sum Fx \quad (5)$$

$$a_0 \sum x^2 + a_1 \sum x^3 + a_2 \sum x^4 = \sum Fx^2 \quad (6)$$

x	x^2	x^3	x^4
-2	4	-8	16
-1	1	-1	1
0	0	0	0
1	1	1	1
2	4	8	16
$\sum x = 0$	$\sum x^2 = 10$	$\sum x^3 = 0$	$\sum x^4 = 34$

In this case we have n=5, then $\sum x = 0$, $\sum x^2 = 10$, $\sum x^3 = 0$ and $\sum x^4 = 34$

Substituting in the above set of simultaneous equation, and then we have

$$a_0(5) + a_1(0) + a_2(10) = \sum F \quad (7)$$

$$a_0(0) + a_1(10) + a_2(0) = \sum Fx \quad (8)$$

$$a_0(10) + a_1(0) + a_2(34) = \sum Fx^2 \quad (9)$$

So, we find that

$$a_0 = \sum F - (5/7)(\sum Fx^2 - 2\sum F)$$

$$a_1 = (\sum Fx)/(\sum x^2) = (\sum Fx)/10$$

and its, digital filter takes the following form:

$$a_1 = \left[-2F_{-2} - F_{-1} + F_1 + 2F_2\right]/10 \quad (10)$$

The term a_1 represent a directional derivative filter that can be running along any direction through the given grid to decipher the tectonic overprint and local litho-structural framework normal to this direction. Generally, at least four maps (N-S, N45^{0}E, N45^{0}W and E-W) could be produced, each of which represents sets of lineaments (system) normal to this direction. by multiply eq. (7) by -2 and add to eq.(9) then we have

$$a_2 = \left\{\sum Fx^2 - 2\sum F\right\}/14$$

$$= \left\{\begin{matrix}\left[4F_{-2} + F_{-1} + F_1 + 4F_2\right] - \\ \left[2F_{-2} + 2F_{-1} + 2F_0 + 2F_1 + 2F_2\right]\end{matrix}\right\}/14 \quad (11)$$

$$a_2 = \left[2F_{-2} - F_{-1} - 2F_0 - F_1 + 2F_2\right]/14 \quad (12)$$

Substitute by eq.(12) in eq.(3) we find the second horizontal derivative (Fxx) in x direction.

$$F_{xx} = 2a_2 = \left[2F_{-2} - F_{-1} - 2F_0 - F_1 + 2F_2\right]/7 \quad (13)$$

The simple form of the second horizontal derivative along profile is [2,-1,-2,-1,2]/7. By the same manner, the second horizontal derivative in Y direction could be computed by using the data of the perpendicular profile.

$$F_{yy} = 2a_2 = \left[2F_{-2} - F_{-1} - 2F_0 - F_1 + 2F_2\right]/7 \quad (14)$$

To calculate the theoretical derivative value, we must include a factor 1/ S^2 where S is the graticule spacing (S). By introducing the factor 1/ S^2 in eq.(13&14) then we get the following:

$$F_{xx} = \left[2F_{-2,0} - F_{-1,0} - 2F_{0,0} - F_{1,0} + 2F_{-2,0}\right]/(7 * S^2)$$
$$= 2\left(2F_{-2,0} - F_{-1,0} - F_{0,0}\right)/\left(7 * S^2\right) \quad (15)$$

$$F_{yy} = \left[2F_{0,-2} - F_{0,-1} - 2F_{0,0} - F_{0,1} + 2F_{0,2}\right]/(7 * S^2)$$
$$= 2\left(2F_{0,-2} - F_{0,-1} - F_{0,0}\right)/\left(7 * S^2\right) \quad (16)$$

|Then the second vertical derivative directly found as

$$F_{zz} = -(F_{xx} + F_{yy}) = (-2/(7 * S^2))\left[(2F_{-2,0} + 2F_{0,-2}) - (F_{-1,0} + F_{0,-1}) - 2F_{0,0}\right] \quad (17)$$

The derived equation can be summarized as

$$F_{zz} = (-2/(7 * S^2))\left[(2F_{-2,0} + 2F_{0,-2}) - (F_{-1,0} + F_{0,-1}) - 2F_{0,0}\right] \quad (18)$$

A set of 5*5 equally spaced data points filter (Fig. 2) could be used to fit the observed data to the plane, but typically, we fit a plane to each (overlapping) set of arrays of 5*5 adjacent points and take the corresponding second vertical derivative values at the midpoint of the corresponding array. Note that not able, with this formula, to compute the first two points at the start and at the end of the run of data we are given.

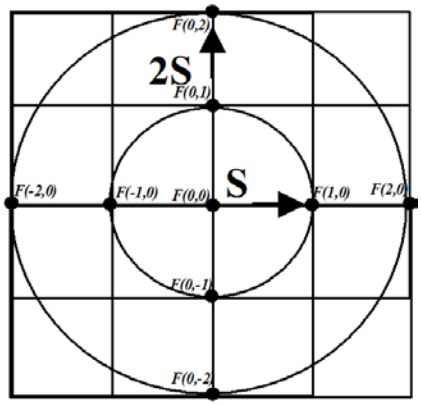

Fig. (2): Horizontal and vertical sets of 5x5 equally spaced data point's filters.

LINEAMENT EXTRACTION

For automatic extraction of a continuous straight lineaments directly form the griddling data file of second vertical derivative (SVD), we developed a very simply algorithm which determine the orientation of a zero contour line in the SVD map by examining the local deviation of zero line in related to the grid cell corners nodes (Fig. 3), The start and end point are calculated as linear function depend on the node values variation in x and y direction.

Length of segment1 is given by the following eq.

$$L_1 = \sqrt{(x_{p_2} - x_{p_1})^2 + (y_{p_2} - y_{1})^2}$$

In other hand, length of segment1 is given by the following eq.

$$L_2 = \sqrt{(x_{p_3} - x_{p_2})^2 + (y_{2} - y_{p_2})^2}$$

LINEAMENTS ANALYSIS

The last algorithm was designed to counting and tabulates the extracted lineaments. The data can be summarized with rose diagrams. It may be representing by graphs in variety ways it either in Number, frequency and/or their ratio.

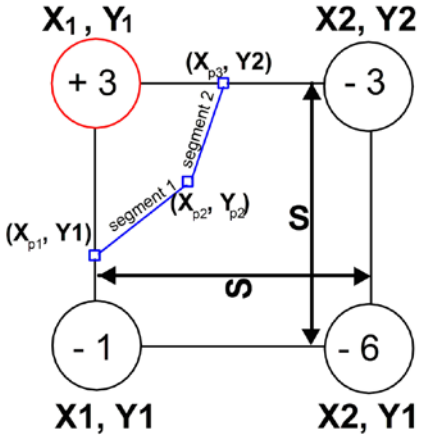

Fig. (3): Show one cell window is used to estimate the lineament orientation and length.

APPLICATIONS (TESTED EXAMPLES)

The proposed method was tested by using theoretical and field examples.

Synthetic Example:

The proposed method was tested by using the well known example described by Cordell (1994). A test model consisting of four right prisms is shown in an isometric view in Figure 4. Light tones indicate positive density contrast; darker tones indicate negative density contrast. Density contrast of the small positive-contrast prism is 0.05 g/cc; density contrast of the other two positive-contrast prisms is +0.01 g/cc, and density contrast of the negative-contrast prism is -0.01 g/cc. The gravity effect of the test model is shown in Figure 5. The different maps of the potential field as obtained by the postulated method are shown in Figure 6. This map was used to resolve the observed data into a number of negative and positive anomalies each of which belong to a certain prism. The result shown in Figure 5 provides a good correspondence between the computed second vertical derivative anomalies and the theoretical models. The contour value of zero delineates carefully the prisms and act as boundaries of the prism.

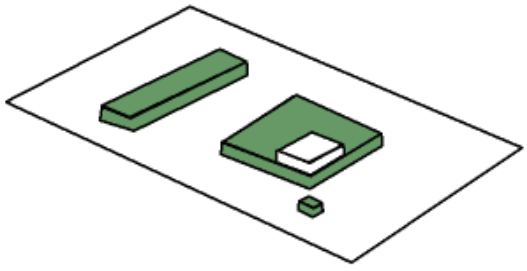

Fig. (4): The isometric view of four prisms test model .

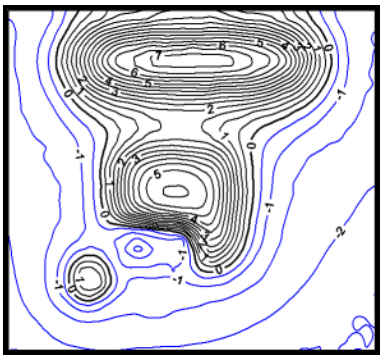

Fig. (5): Gravity effects of prism models of Figure 4. Contourinterval is 0.5 mgal.

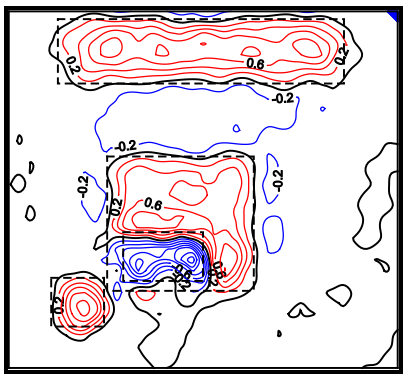

Fig. (6): The computed second vertical derivative. Dashed lines represent the prisms outlines

FIELD EXAMPLE

1- The Thomas Landfill Site Case Study:

The gravity method is potentially useful in landfill studies because the waste deposit is usually less dense than the enclosing medium (Roberts, et. al. 1991). The Bouguer anomaly of Thomas Farm Landfill (Fig. 7) was used as a tested example. By application of the new equation, the calculated second vertical derivative map (Fig. 8) has negative and positive parts. The negative part delineates carefully landfill zone and the dashed blue line represent the outer boundaries of the landfill zone.

2- Field Example

EL-Kharga area (Fig. 9) was selected to test the validity of this technique. The chosen area comprises the Southern part of the Western Desert of Egypt, between lat. 24^0 38’ 07”N & 25^0 40 ‘ 30” N and long. 30^0 28’ 00” E & 30^0 46’ 00” E. Many authors believe that these depressions were the result of wind action as a main eroding agent together with the climatic changes and heavy rains.

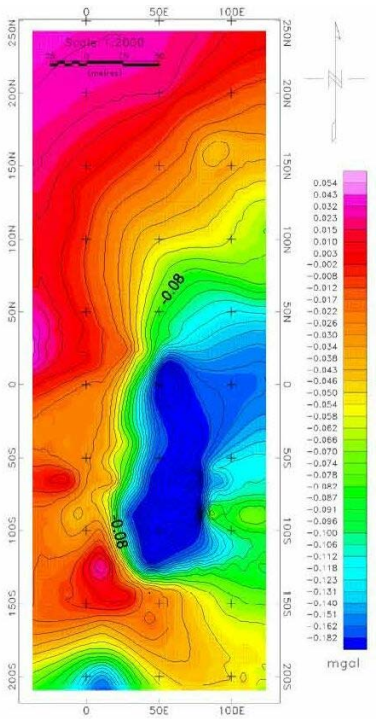

Fig. (7): Bouguer gravity anomaly contour map of the Thomas Farm Landfill (Roberts, et al., 1991).

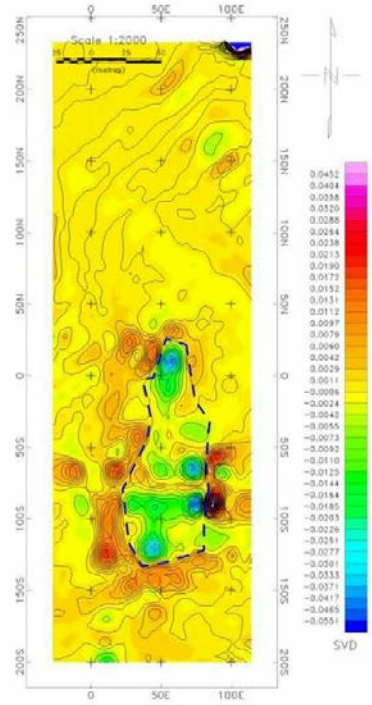

Fig. (8): The computed SVD map of the Thomas Farm Landfill the dashed blue line represents the outer boundaries of the landfill Zone.

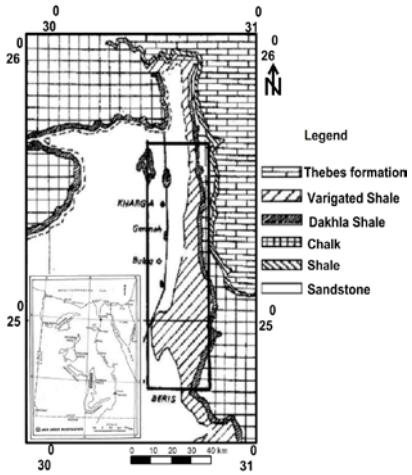

Fig. (9): Geological map of Kharga Oasis (After Said, 1962)

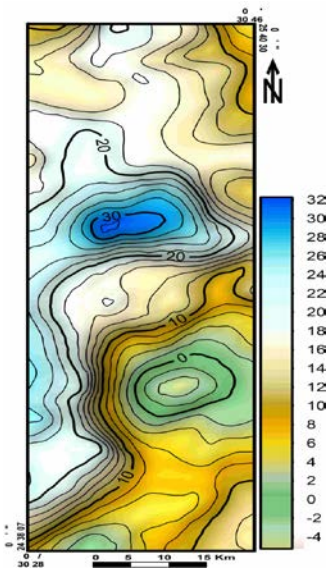

Fig. (10): Bouguer anomaly map.

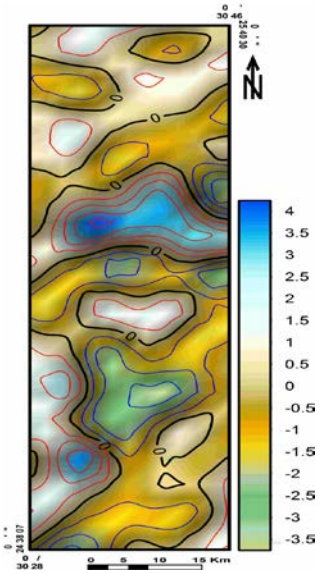

Fig. (11): Second Vertical Derivative map.

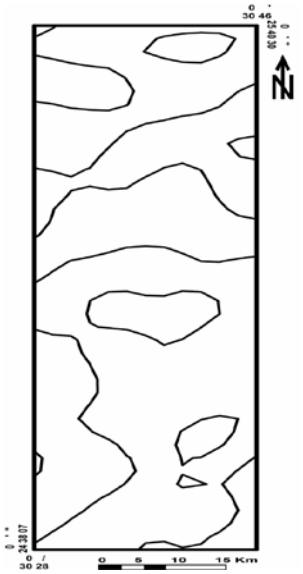

Fig. (12): Extracted lineaments.

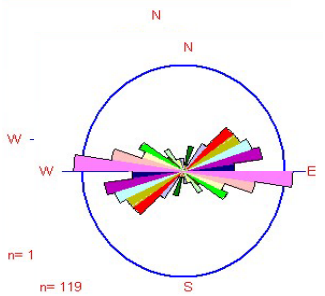

(a)

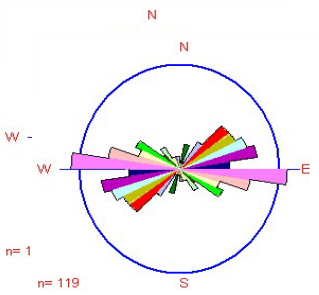

(b)

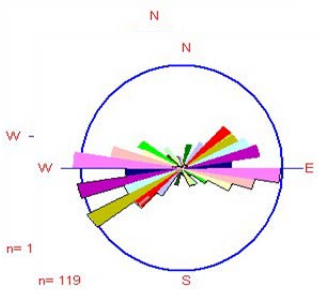

(c)

Fig. (13): Rose diagrams of the structural lineaments (a) Number wise (b) Length wise and (c) Ratio.

The Bouguer-anomaly map of Kharga area was compiled by (GEOFIZIKA, 1961) was constructed (El-Ghalban, 1980) with contour interval 1 mGal. The authors returned to this gravity data in order to ascertain whether more careful work could detect the anomaly expected from the formations known to be present. Figure(10) is the resulting Bouguer anomaly map of the area of interest Contour interval is 1 mGal. Figure (11), second vertical derivative map as calculated from the proposed equation.

Figure 12 shows the extracted lineaments. Figure 13 shows the main directional trends of extracted lineaments based on their number, length and ratio. The analyses of these faults indicated that most of the well-developed structural lineaments have NE-SW to ENE-WSW and ESE-WNW to E-W trends.

CONCLUSION

The traditional identification and interpretation of lineaments is subjective and inefficient. It depends on the map quality, contour interval, and interpreter's judgment. To overcome these limitations, we proposed automatic detection and extraction of lineament features directly from geophysical data. Three algorithms were used to accomplish these goals.

The proposed method is tested using theoretical and field examples. Through tests with synthetic and with real data from EL-Kharga area in southern western desert of Egypt, the detection and extraction methods are shown to be more effective than the conventional applications. The results from the real data roughly coincide with major geologic faults that are visually identified. These results show that the methods constitute a useful tool to aid fault interpretation.

REFERENCES

Abdelrahman, E.M. and El-araby, H.M. (1988): "Optimum Second Derivative Coefficient Set For Various Grid System". E.G.S. Vol. 6, pp. 44-53.

Agarwal, B.N.P., and Lal, T., 1972a, Calculation of the vertical gradient of the gravity field using the Fourier transform: Geophys. Prosp., 20, 448-458.

Agarwal, B.N.P., and Lal, T., 1972b, A generalized method of computing second derivatives of gravity fields: Geophys. Prosp., 20, 385-394.

Agocs, W.B., 1951: "Least square residual anomaly determination:, Geophysics V. 36: pp 571-581.

Baranov, W., 1975, Potential fields and their transformations in applied geophysics: Geoexpl. Mono., Series I-No. 6, Geopublication Assoc.

Beyer, L.A., 1971, The vertical gradient of gravity in vertical and near-vertical boreholes: Open File Report 71-42, U. S. Geol. surv.

Butler, D.K., 1983, Microgravimetry and the theory, measurement, and application of gravity gradients: Ph.D. dissertation, Texas A&M University.

Butler, D.K., 1984a, Interval gravity-gradient determination concepts: Geophysics, 49, 828-832.

Butler, D.K., 1984b, Microgravimetric and gravity gradient techniques for detection of subsurface cavities: Geophysics, 49, 1084-1096.

Cordell, L. 1994: "Potential-field sounding using Euler's homogeneity equation and Zidarov bubbling". Geophysics, Vol.59,No. 6; p. 902-908.

Darby, E.K., and Davies, E.B., 1967: "The analysis and design of two-dimensional fitters for two-dimensional data": Geophys. Prosp.. Y. 15, p. 383-406.

Dean, W.C., 1958: "Frequency analysis for gravity and magnetic interpretation": Geophysics, v. 23, p. 97-127.

Elkins, T.A., 1951: "The second derivative method of gravity-interpretation": Geophysics, v. 16, p. 29-50.

Evjen, H.M., 1936: "The place of the vertical gradient in gravitational interpretation": Geophysics, v. I, p. 127-136.

Evjen, H.M., 1936, The place of the vertical gradient in gravitational interpretations: Geophysics, 1, 127-136.

Fajklewicz, Z.J., 1976, Gravity vertical gradient measurements for the detection of small geologic and anthropomorphic forms: Geophysics, 41, 1016-1030.

Fuller. B.I., 1967: "Two-dimensional frequency analysis and design of grid operators", in Mining Geophysics, v. II: SEG, Tulsa. p. 658-708.

Geosoft Inc., 1999, GM-SYS modeling of potential field data. Geosoft Inc., Toronto, Canada.

Green, R., 1976, Accurate determination of the dip angle of a geological contact using the gravity method: Geophys. Prosp., 24, 265-272.

Hammer, S., and Anzoleaga, R., 1975, Exploring for stratigraphic traps with gravity gradients: Geophysics, 40, 256-268.

Heiland, C. A., 1943, A rapid method for measuring the profile components of horizontal and vertical gravity gradients: Geohysics, 8, 119-133.

Henderson R.G., and Zietz, I., 1949: "The computation of second vertical derivative of geomagnetic fields": Geophysics, 14, 290-319.

Khamies A., El-Terb A., El-sadek M., 2001: Application of directional derivative filter in the determination of aeromagnetic lineaments.

Klingele, E.E., Marson, I., and Kahle, H.G., 1991, Automatic interpretation of gravity gradiometric data in two dimensions-Vertical gradient: Geophys. Prosp., 39, 407-434.

Moon, W.M., Ushah, A., Singh, V., Bruce, B., 1988, Application of 2-D Hilbert transform in geophysical imaging with potential field data: IEEE Trans. on Geoscience and Remote Sensing, 26, 502-510.

Mueller, I.I., 1960, The gradients of gravity and their applications in geology: Ph.D. dissertation, Ohio State University.

Nabighian, M.N., 1984: Toward a three-dimensional automatic interpretation of potential field data via generalized Hilbert transforms-Fundamental relations: Geophysics, 49, 780-786.

Nettleton, L.L., 1976: "Gravity and Magnetic in Oil prospecting" Mc-Graw Hill Book, London.

Pederson, L.B., 1989, Relations between horizontal and vertical gradients of potential fields: Geo

Peters, L.J. 1949: "The direct approach to magnetic interpretation and its practical application". Geophysics v.14, 290-319.

Rosenbach, O., 1953: "A contribution to the computation of the second derivative from gravity data". Geophysics, v. 18, p. 894-912

Rowan, L.C. and Lathran, E.H., 1980: Mineral Exploration: in Remote Sensing in Geology, Siegel, B.S., and Gillespie, A. R.,Eds., Wiley, New York, p. 553-605.

Shuey, R.T., 1972, Applications of physics, 54, 662-663.

Stanley, J.M., 1977, Simplified gravity interpretation by gradients- The geologic contact: Geophysics, 42, 1230-1235.

Stanley, J.M. and Green, R., 1976, Gravity gradients and the interpretation of the truncated plate: Geophysics, 41, 1370-1376.

Talwani, M. and Heirtzler, J.R., 1964, Computation of magnetic anomalies caused by two-dimensional bodies of arbitrary shape, in Parks, G. A., Ed., Computers in the mineral industries, Part 1: Stanford Univ. Publ., Geol. Sci., Vol. 9, pp. 464-480.

Talwani, M., Worzel, J. L., and Landisman, M., 1959, Rapid gravity computations for two-dimensional bodies with application to the Mendocino submarine fracture zone: Jour. Geophys. Res., Vol. 64, pp. 49-59.

Trommer, R., 1964, Der gravimetrische Vertikalgradient: Leipzig, Freiberger Forchungshefte, C175.

Zhang L., Wu J., Hao T. and Wang J., (2006): Automatic lineament extraction from potential-field images using the Radon transform and gradient calculation. Geophysics vol. 71, n°3, p. 31-40.